Washington University School of Medicine
Digital Commons@Becker

Open Access Publications

2017

Nuclear export factor 3 regulates localization of small nucleolar RNAs

Melissa W. Li
Washington University School of Medicine in St. Louis

Arthur C. Sletten
Washington University School of Medicine in St. Louis

Jiyeon Lee
Washington University School of Medicine in St. Louis

Kelly D. Pyles
Washington University School of Medicine in St. Louis

Scot J. Matkovich
Washington University School of Medicine in St. Louis

See next page for additional authors

Follow this and additional works at: https://digitalcommons.wustl.edu/open_access_pubs
Please let us know how this document benefits you.

Recommended Citation

Li, Melissa W.; Sletten, Arthur C.; Lee, Jiyeon; Pyles, Kelly D.; Matkovich, Scot J.; Ory, Daniel S.; and Schaffer, Jean E., "Nuclear export factor 3 regulates localization of small nucleolar RNAs." Journal of Biological Chemistry. 292, 49. 20228-20239. (2017).
https://digitalcommons.wustl.edu/open_access_pubs/6478

This Open Access Publication is brought to you for free and open access by Digital Commons@Becker. It has been accepted for inclusion in Open Access Publications by an authorized administrator of Digital Commons@Becker. For more information, please contact vanam@wustl.edu.

Authors

Melissa W. Li, Arthur C. Sletten, Jiyeon Lee, Kelly D. Pyles, Scot J. Matkovich, Daniel S. Ory, and Jean E. Schaffer

This open access publication is available at Digital Commons@Becker: https://digitalcommons.wustl.edu/open_access_pubs/6478

Nuclear export factor 3 regulates localization of small nucleolar RNAs

Received for publication, September 16, 2017, and in revised form, October 5, 2017 Published, Papers in Press, October 11, 2017, DOI 10.1074/jbc.M117.818146

Melissa W. Li[‡], Arthur C. Sletten[‡], Jiyeon Lee[‡], Kelly D. Pyles[‡], Scot J. Matkovich[§], Daniel S. Ory[‡], and Jean E. Schaffer[‡1]

From the [‡]Diabetes Research Center, Department of Medicine, and [§]Center for Cardiovascular Research, Department of Medicine, Washington University School of Medicine, St. Louis, Missouri 63110

Edited by Ronald C. Wek

Small nucleolar RNAs (snoRNAs) guide chemical modifications of ribosomal and small nuclear RNAs, functions that are carried out in the nucleus. Although most snoRNAs reside in the nucleolus, a growing body of evidence indicates that snoRNAs are also present in the cytoplasm and that snoRNAs move between the nucleus and cytoplasm by a mechanism that is regulated by lipotoxic and oxidative stress. Here, in a genome-wide shRNA-based screen, we identified nuclear export factor 3 (NXF3) as a transporter that alters the nucleocytoplasmic distribution of box C/D snoRNAs from the ribosomal protein L13a (*Rpl13a*) locus. Using RNA-sequencing analysis, we show that NXF3 associates not only with *Rpl13a* snoRNAs, but also with a broad range of box C/D and box H/ACA snoRNAs. Under homeostatic conditions, gain- or loss-of-function of NXF3, but not related family member NXF1, decreases or increases cytosolic *Rpl13a* snoRNAs, respectively. Furthermore, treatment with the adenylyl cyclase activator forskolin diminishes cytosolic localization of the *Rpl13a* snoRNAs through a mechanism that is dependent on NXF3 but not NXF1. Our results provide evidence of a new role for NXF3 in regulating the distribution of snoRNAs between the nuclear and cytoplasmic compartments.

Small nucleolar RNAs (snoRNAs)[2] are a class of non-coding RNAs that range from 60 to 250 nucleotides in length. In mammalian cells, the majority of snoRNAs are encoded within introns and processed from lariats during splicing. snoRNAs assemble into small nucleolar ribonucleoprotein (snoRNP) complexes with RNA-modifying enzymes and traffic to the nucleolus, where their canonical function is to guide site-specific nucleotide modifications of rRNA and snRNA. Two classes of snoRNAs are defined by conserved sequence motifs, associated proteins, and snoRNA-directed modifications. Box C/D snoRNAs complex with fibrillarin and guide 2′-*O*-methylation of targets, whereas box H/ACA snoRNAs complex with dyskerin and guide pseudouridylation of targets (1–3). In addition to these canonical roles, there is growing evidence for non-canonical molecular functions of snoRNAs, including miRNA-like post-transcriptional regulation, pseudouridylation of mRNA targets, modification of pre-mRNAs to direct splicing, and regulation of RNA editing (4–7).

Our laboratory previously identified that box C/D snoRNAs encoded within the introns of the ribosomal protein L13a (*Rpl13a*) gene are critical mediators of the cellular response to palmitate-induced lipotoxic stress and play a physiological role in tissue responses to oxidative stress (8–10). Although *Rpl13a* snoRNAs localize primarily in the nucleus, these and other snoRNAs are readily detected in the cytoplasm under homeostatic conditions (11, 12), and they accumulate outside the nucleus during lipotoxic conditions, oxidative stress, and serum starvation (8, 10, 13). In addition to the pathways for nuclear export of snoRNAs implicated by these findings, studies in *Xenopus* oocytes provide evidence for an endogenous pathway that transports snoRNAs from the cytoplasm to the nucleus following microinjection (14). Moreover, U8 snoRNA associates with the import factor snurportin 1 in mammalian cells, and knockdown of this transport adaptor is associated with increased cytoplasmic U8 (11). Whether snurportin 1 serves a broader role in transport of the overall class of snoRNAs and whether other transport proteins function to regulate the distribution of snoRNAs between the nucleus and cytoplasm is not known.

We identified nuclear export factor 3 (NXF3) through an shRNA loss-of-function genetic screen in human umbilical vein endothelial cells to identify genes required for the cytotoxic response to metabolic stress. Based on sequence similarity, NXF3 is considered to be a member of a nuclear RNA export factor family that includes the known mRNA exporter, nuclear export factor 1 (NXF1). Like other family members, NXF3 shuttles between the nucleus and cytoplasm and can associate with and transport poly(A)$^+$ RNA (15). Given that our genetic screens implicated both snoRNAs and NXF3 in lipotoxic response pathways, we hypothesized that NXF3 may also serve as a transporter for snoRNAs. Herein, we demonstrate that NXF3 regulates distribution of the *Rpl13a* snoRNAs between the nucleus and the cytosol under homeostatic conditions.

This work was supported by National Institutes of Health Grants R01 DK064989, P30 DK020579, and T32 HL007275 and by American Heart Association Grant 15PRE25220014. The authors declare that they have no conflicts of interest with the contents of this article. The content is solely the responsibility of the authors and does not necessarily represent the official views of the National Institutes of Health.

Sequence data have been deposited in NCBI's Gene Expression Omnibus (accession number GSE106301).

[1] To whom correspondence should be addressed: Washington University School of Medicine, 660 South Euclid Ave., Campus Box 8086, St Louis, MO 63110. Tel.: 314-362-8717; Fax: 314-747-0264; E-mail: jschaff@wustl.edu.

[2] The abbreviations used are: snoRNA, small nucleolar RNA; snoRNP, small nucleolar ribonucleoprotein; HUVEC, human umbilical vein endothelial cell; qPCR, quantitative PCR; NPM, nucleophosmin; DOX, doxorubicin; ROS, reactive oxygen species; DHE, dihydroethidium.

© 2017 by The American Society for Biochemistry and Molecular Biology, Inc. Published in the U.S.A.

Downloaded from http://www.jbc.org/ at Washington University on January 5, 2018

NXF3 associates with a broad array of box C/D and box H/ACA snoRNAs, including the *Rpl13a* snoRNAs. Treatment of cells with the adenylyl cyclase activator forskolin decreases cytosolic snoRNAs through a mechanism that is dependent on NXF3 expression. Our data provide new insights into the molecular regulation of snoRNA localization.

Results

Knockdown of NXF3 protects against lipotoxic cell death in endothelial cells

To identify genes critical for the cell death response to lipotoxicity, we performed a genome-wide loss-of-function shRNA screen in immortalized human umbilical vein endothelial cells (HUVECs), which are sensitive to lipotoxicity. Cells were transduced with seven pools of lentivirus, each containing ~10,000 unique shRNAs targeting expressed human genes and a puromycin selectable marker. As a control, cells were transduced in parallel with a non-silencing shRNA virus that has no homology to known mammalian genes. HUVECs that survived puromycin selection were then treated for 48 h in media supplemented with pathophysiological levels of palmitic acid to model lipotoxic conditions. Compared with cells transduced with the non-silencing control shRNA, cells transduced with an shRNA targeting NXF3 demonstrated less induction of markers of endoplasmic reticulum stress, an early feature of the lipotoxic response (Fig. 1*A*). Furthermore, cells with the NXF3-targeting shRNA had improved viability under lipotoxic conditions (Fig. 1*B*). The shRNA targeting NXF3 led to a 72% decrease in NXF3 mRNA levels (Fig. 1*C*) and a 31% decrease in NXF3 protein expression (Fig. 1*D*), consistent with knockdown of its gene target in these lipotoxicity-sensitive human cells. NXF3 is a member of the NXF family that includes the general mRNA export receptor, NXF1. Our shRNA library included shRNAs that target NXF1, but cells transduced with NXF1-targeting shRNA or shRNA targeting other known RNA transporters did not survive the palmitate selection. Together these observations implicate a critical role for NXF3, but not NXF1, in the lipotoxic response pathway.

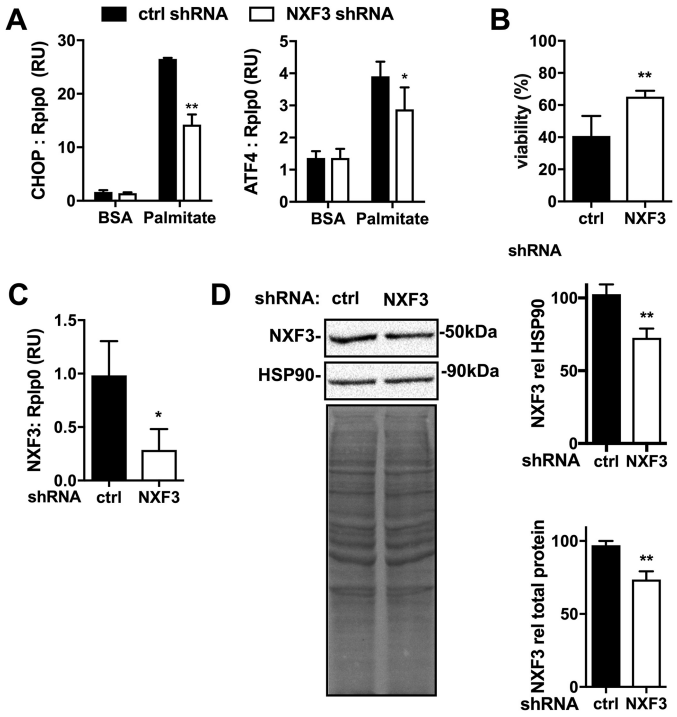

Figure 1. Knockdown of NXF3 protects against lipotoxic cell death in endothelial cells. HUVECs were transduced with non-targeting (*ctrl*) or NXF3-targeting shRNA. *A,* quantification of ER stress markers (*CHOP* and *ATF4*) by RT-qPCR relative to Rplp0 (relative units, *RU*) following 4 h of incubation in media containing 500 μM palmitate. $n = 3$ independent experiments. *B,* viability following 48 h of incubation in media containing 500 μM palmitate. $n = 4$. *C,* RT-qPCR quantification of NXF3 mRNA relative to Rplp0. $n = 3$. *D,* representative Western blot analysis of NXF3 and HSP90 expression (*top panels*) and corresponding Ponceau-stained gel (*bottom panel*). *Graphs* report quantification of NXF3 expression relative to HSP90 or total protein from $n = 3$. Means ± S.D. *, $p < 0.05$; **, $p < 0.01$ for NXF3 knockdown *versus* control.

NXF3 knockdown endothelial cells have aberrant Rpl13a snoRNA localization

Although NXF3 can associate with mRNAs, other potential cargo such as non-coding RNAs has not been investigated (16). Given the important role of *Rpl13a* snoRNAs U32a, U33, U34, and U35a in lipotoxic and oxidative stress-induced cell death and the observation that these snoRNAs accumulate in the cytoplasm under metabolic stress conditions (8, 10), we hypothesized that NXF3 knockdown might affect localization of snoRNAs. We assessed *Rpl13a* snoRNA localization in cytosolic fractions of control- and NXF3-shRNA-transduced cells by isolating cytosolic and non-cytosolic fractions using digitonin extraction. Under normal homeostatic growth conditions, levels of cytosolic *Rpl13a* snoRNAs in NXF3 shRNA-transduced cells were significantly increased compared with control shRNA-transduced cells, even though total cellular abundance for these snoRNAs was unchanged (Fig. 2*A*). Western blottings demonstrated that both nuclear (nucleophosmin) and cytosolic (HSP90, α-tubulin) markers segregated as expected in both control and NXF3 shRNA-transduced cells (Fig. 2*B*). Consistent with prior observations in other cell types that oxidative stress stimulates cytosolic accumulation of *Rpl13a* snoRNAs (8, 17), U32a, U33, and U34 snoRNAs accumulate in the cytoplasm of control shRNA-transduced HUVECs in response to treatment with hydrogen peroxide (Fig. 2*C*). Hydrogen peroxide had no detectable effect on localization of U35a, which is the least abundant of the *Rpl13a* snoRNAs and shows less robust cytosolic accumulation in response to other metabolic stress inducers (8). In NXF3 shRNA-transduced cells, hydrogen peroxide did not cause further increase in the cytoplasmic levels of *Rpl13a* snoRNAs. Elevated cytoplasmic levels of the snoRNAs under homeostatic conditions in NXF3 shRNA-transduced cells are unlikely to be the result of increased basal oxidative stress, because intracellular hydrogen peroxide levels as assessed by dihydroethidium staining were unchanged compared with control cells (Fig. 2*D*). Nucleophosmin staining showed preservation of discrete nucleolar foci in NXF3 shRNA-transduced cells, in contrast to the diffuse nucleophosmin staining characteristic of nucleolar stress in hydrogen peroxide-treated cells (Fig. 2*E*), indicating that NXF3 knockdown does not cause nucleolar stress (18). Our findings that loss-of-function of NXF3 perturbs *Rpl13a* snoRNA subcellular localization indicates that NXF3 functions under homeostatic conditions to maintain the distribution of these non-coding RNAs between the nucleus and cytoplasm. Although NXF3 has been proposed

Downloaded from http://www.jbc.org/ at Washington University on January 5, 2018

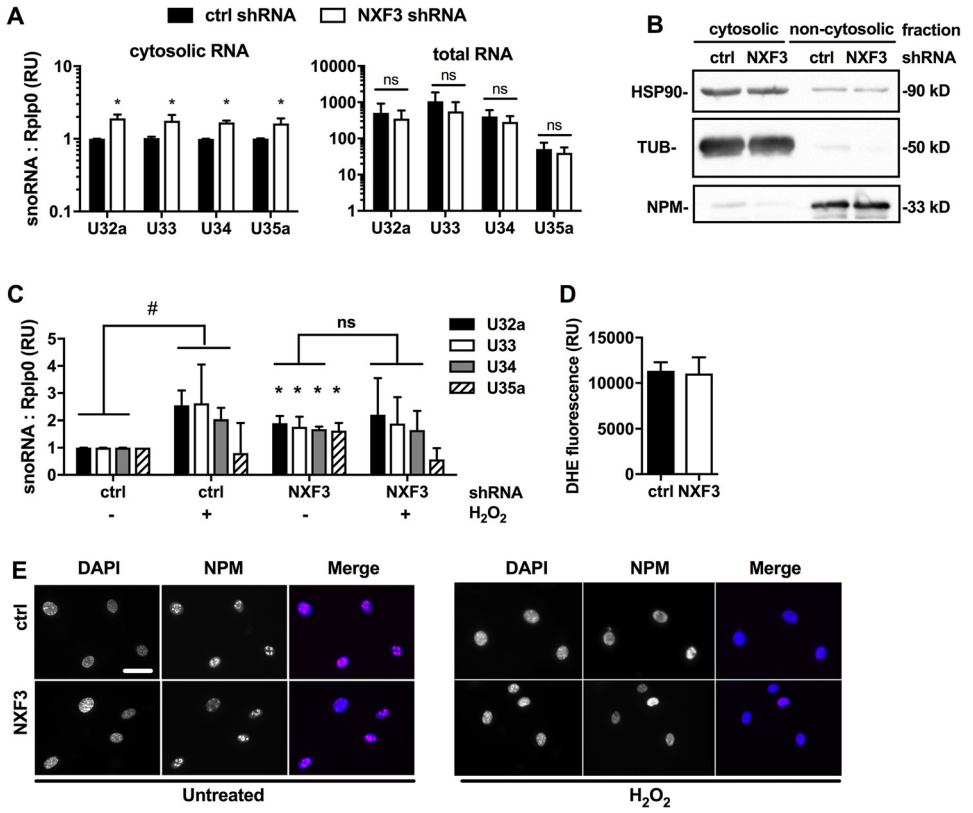

Figure 2. NXF3 knockdown alters *Rpl13a* snoRNA localization under basal growth conditions in endothelial cells. HUVECs were transduced with control (*ctrl*) or NXF3-targeting shRNA. *A,* RT-qPCR quantification of *Rpl13a* snoRNAs (relative to Rplp0) in cytosolic (*left graph*) or total extracts *(right graph*). $n = 4$. *B,* representative Western blot analysis of cytosolic and non-cytosolic fractions for cytosolic (HSP90; α-tubulin, *TUB*) and nuclear (nucleophosmin, *NPM*) markers. *C,* cells were untreated or treated with 1 mM H_2O_2 for 4 h. RT-qPCR quantification of *Rpl13a* snoRNAs in cytoplasm relative to Rplp0 and normalized to levels in untreated control shRNA-transduced cells. $n = 3$. *D,* quantification of superoxide in untreated control and NXF3-knockdown cells by DHE staining. $n = 3$ independent experiments, each sample containing 10^4 cells. *E,* representative immunofluorescence staining for NPM in untreated and H_2O_2-treated cells. Nuclei stained with DAPI. *Scale bar,* 50 μM. Means ± S.D. *, $p < 0.05$ for NXF3 *versus* control shRNA-transduced cells; #, $p < 0.05$ for H_2O_2-treated *versus* -untreated; *ns*, non-significant.

as an mRNA export factor, accumulation of *Rpl13a* snoRNAs in the cytosol in the setting of NXF3 knockdown implicates an additional role for this protein in nuclear import of these small non-coding RNAs.

NXF3 and NXF1 associate with snoRNAs

Because NXF3 is a member of a nuclear RNA transporter family, and genetic manipulation of NXF3 impacted *Rpl13a* snoRNA localization, we hypothesized that NXF3 may serve as a snoRNA transporter. To further elucidate the effects of NXF3 on snoRNA localization, we used NIH3T3 murine fibroblasts and H9c2 rat cardiomyoblasts, cell types that are also sensitive to lipotoxicity but grow more rapidly in cell culture and transfect with greater efficiency than HUVECs (8, 10, 19). To test whether NXF3 physically interacts with the *Rpl13a* snoRNAs, we transiently transfected NIH3T3 fibroblasts with NXF3-GFP or GFP alone as a negative control. We also transfected cells with NXF1-GFP, another NXF family member with related domain structure (Fig. 3*A*). We performed immunoprecipitations using a GFP antibody or non-immune IgG as a control. Antibody directed against GFP efficiently and specifically pulled down NXF3-GFP, NXF1-GFP, or GFP, whereas no NXF3-GFP, NXF1-GFP, or GFP was recovered in control immunoprecipitations (Fig. 3*B*). Real-time PCR quantification revealed a 9–12-fold increase in *Rpl13a* snoRNA association with immunoprecipitated NXF3-GFP compared with immunoprecipitated GFP (Fig. 3*C*). Unexpectedly, the *Rpl13a* snoRNAs also associated with NXF1-GFP. These data indicate that under mild detergent conditions chosen to preserve RNA–protein interactions, both NXF3-GFP and NXF1-GFP associate with the *Rpl13a* snoRNAs. This may reflect an ability of these transporters to bind a broad range of RNA species.

We used RNA-sequencing to determine whether NXF3 associates only with *Rpl13a* snoRNAs or with snoRNAs more broadly. We collected RNA from cell lysates before immunoprecipitation (input) and RNA from immunoprecipitates (pulldown) of NIH3T3 murine fibroblasts transfected with NXF3-GFP. Because most snoRNAs lack poly(A) tails and do not efficiently prime with random hexamers, they are not well-represented in libraries prepared using approaches suitable for larger RNAs (20). To achieve broad coverage of snoRNAs from both input and pulldown samples, we size-selected RNAs from 30 to 375 nucleotides, a range that would exclude most miRNAs and include most snoRNAs. Libraries were prepared using an Illumina small RNA library preparation kit, sequenced, and aligned to mm9 Refseq Transcripts. We focused our analyses on the non-rRNA sequences, which accounted on average for 55% reads in both input and pulldown samples (Table 1). Greater than 98% of non-rRNA reads in the input and pulldown

Downloaded from http://www.jbc.org/ at Washington University on January 5, 2018

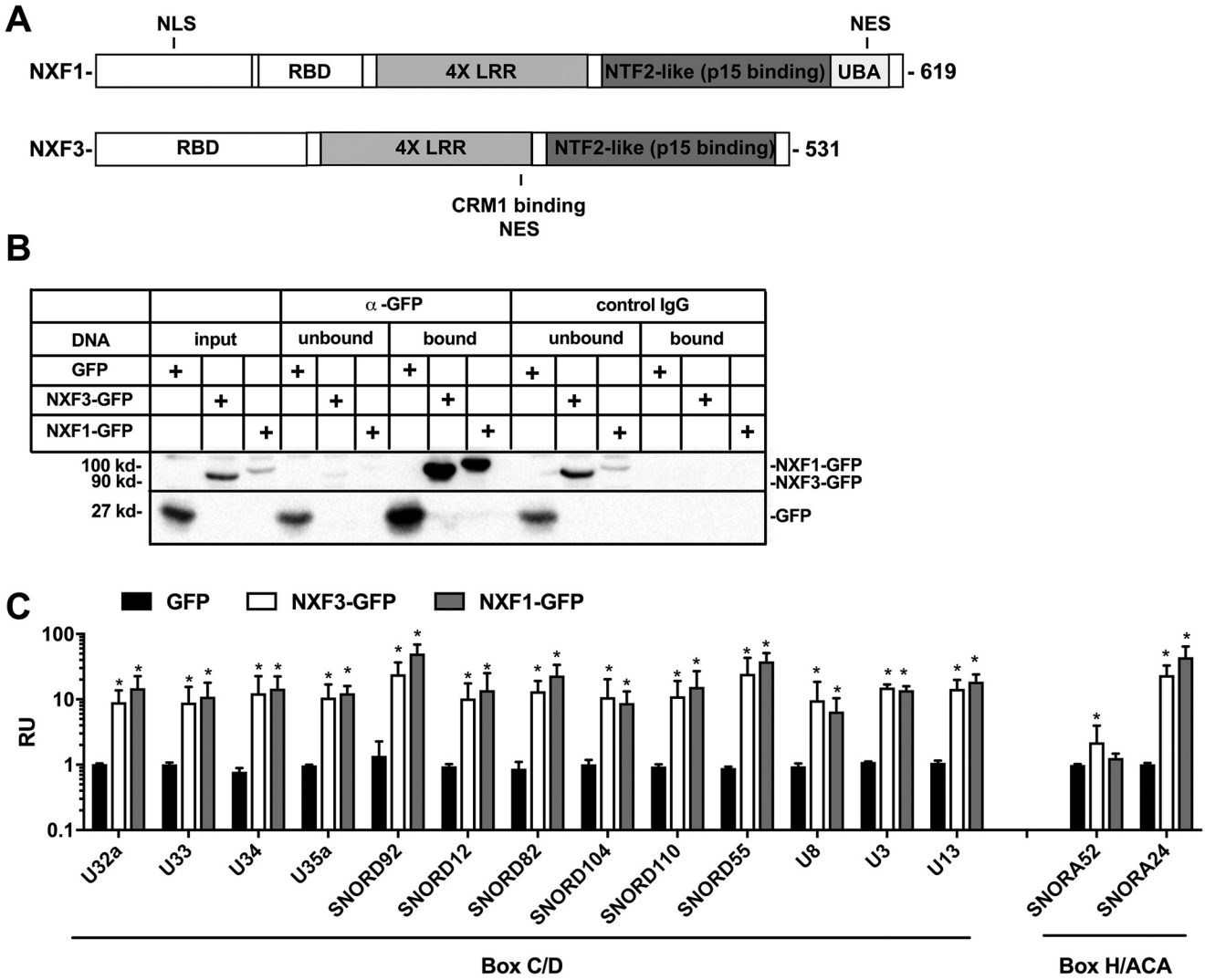

Figure 3. snoRNAs associate with NXF proteins. *A,* domain structures of NXF1 and NXF3 showing RNA-binding domain (*RBD*), four leucine-rich repeat domain (*4× LRR*), sequence with similarity to nuclear transport factor 2 (*NTF2-like* (*p15 binding*)), ubiquitin-associated-like domain (*UBA*), nuclear localizing sequence (*NLS*), nuclear export sequence (*NES*), and CRM1-binding region. *B* and *C,* NIH3T3 fibroblasts were transfected with control plasmid (*GFP*) or plasmid encoding NXF3-GFP or NXF1-GFP. Immunoprecipitation with α-GFP or rabbit IgG (*control*) was analyzed by Western blot analysis using α-GFP (*B*). Co-immunoprecipitating RNA was quantified by RT-qPCR for *Rpl13a* snoRNAs and selected box C/D and box H/ACA snoRNAs. *Graphs* (*C*) report enrichment in NXF3-GFP- or NXF1-GFP-transfected cells over GFP-transfected cells. Means ± S.D. for $n = 3$. *, $p < 0.05$ for NXF3-GFP- or NXF1-GFP-transfected *versus* GFP-transfected.

Table 1
Quality of RNA sequencing data

	Total reads	Avg. quality	% G/C	Total aligned	% aligned	% rRNA
Input 1	12622611	36.56	42.81	6914155	54.78	49.32
Input 2	8494636	36.53	43.23	3561964	41.93	36.13
Input 3	15845764	36.57	42.99	7717165	48.70	42.95
Pulldown 1	3321562	36.63	43.40	1498556	45.12	38.85
Pulldown 2	19470767	36.55	42.52	12639529	64.92	59.51
Pulldown 3	13412207	36.55	42.45	6330452	47.20	43.59

Table 2
Distribution of non-ribosomal RNA reads
NS means not significant.

RNA	Input	Pull down	Significance
	%	%	
C/D snoRNA	92.45 ± 0.93	91.92 ± 1.69	NS
H/ACA snoRNA	6.26 ± 0.79	6.98 ± 1.50	NS
lncRNA	0.24 ± 0.04	0.33 ± 0.08	NS
miRNA	0.27 ± 0.02	0.19 ± 0.07	NS
mRNA	0.76 ± 0.09	0.59 ± 0.13	NS
Other	0.02 ± 0.00	0.00 ± 0.00	NS

samples aligned to snoRNAs, as expected (Table 2). In addition to the *Rpl13a* snoRNAs, NXF3 pulldown recovered many other snoRNAs (Table 3), most of which belonged to the box C/D class of snoRNAs, known to be most abundant (21–23). Approximately 6% of reads in both input and pulldown aligned to box H/ACA snoRNAs. Because of the methods required to capture snoRNA sequences in library preparation, it was not possible to determine whether NXF3 specifically enriches for snoRNAs over other classes of RNAs. Nonetheless, the lack of significant enrichment of specific snoRNA species in pulldown relative to input snoRNAs indicates that NXF3 broadly associates with this class of small RNAs and does not have specificity for the *Rpl13a* snoRNAs or other particular species (Table 3).

To validate association of NXF3 with additional box C/D and box H/ACA snoRNAs and to test whether NXF1 also interacted

Downloaded from http://www.jbc.org/ at Washington University on January 5, 2018

Table 3
Most abundant immunoprecipitating snoRNAs
FDR means false discovery rate, and NS means not significant.

Gene ID	LS mean (pull down)	LS mean (input)	Enrichment (pull down/input)	FDR	*p* value	Significance
Snord55	421533.33	422930.00	1.00	1.00	0.84	NS
Snord44	299548.00	218320.33	1.37	0.99	0.87	NS
Z23	229492.67	218334.00	1.05	0.99	0.56	NS
Snord24	208143.67	156536.67	1.33	0.99	0.90	NS
Snord2	144321.67	150285.33	0.96	1.00	0.64	NS
Snora48	120987.00	114743.00	1.05	0.99	0.87	NS
Snord45	97189.00	82084.33	1.18	0.99	0.77	NS
Z19	76795.67	86895.67	0.88	0.99	0.57	NS
Z15	70041.33	78718.67	0.89	0.99	0.64	NS
Snord14e	56763.00	51011.67	1.11	0.99	0.90	NS
Snord4a	50187.00	32887.00	1.53	1.00	0.91	NS
Snord96a	29898.00	36448.00	0.82	1.00	0.53	NS
Snord45c	26526.00	17509.67	1.51	0.99	0.99	NS
Snord74	23828.33	20331.67	1.17	0.99	0.74	NS
Snord32a	23639.33	36071.67	0.66	1.00	0.62	NS
Snord14d	18182.33	14849.67	1.22	0.99	0.79	NS
Snord14c	14650.00	11996.67	1.22	0.99	0.77	NS
Snord73	11345.33	10193.33	1.11	0.99	0.61	NS
Snord34	10821.67	9770.33	1.11	1.00	0.61	NS
Snord95	9882.33	7793.67	1.27	1.00	0.84	NS
Snord1b	8164.00	8715.67	0.94	1.00	0.49	NS
Snord35a	5050.33	7777.33	0.65	1.00	0.43	NS
Snord113	4508.67	5383.67	0.84	0.99	0.81	NS
Snord82	4491.33	3655.33	1.23	1.00	0.97	NS
Snord104	3567.00	2764.67	1.29	1.00	0.98	NS
DQ267100	2406.67	3323.33	0.72	0.99	0.50	NS
Snord100	2392.67	2097.33	1.14	1.00	0.76	NS
Snord1c	2302.00	2378.67	0.97	1.00	0.42	NS
Snord12	2044.33	862.67	2.37	1.00	0.34	NS
Snord33	1497.33	881.00	1.7	1.00	0.87	NS
Snord15b	1280.00	1128.67	1.13	1.00	0.99	NS
Snord123	1268.67	1322.00	0.96	1.00	0.45	NS
Rnu73b	980.33	984.00	1.00	1.00	0.47	NS
DQ267102	963.33	1123.33	0.86	0.99	0.74	NS
Snord92	746.67	466.00	1.60	1.00	0.88	NS
Snord37	650.00	674.67	0.96	0.99	0.61	NS
AF357426	647.33	366.67	1.77	0.99	0.98	NS
AF357425	505.67	525.67	0.96	0.99	0.81	NS
Snord15a	478.00	545.67	0.88	1.00	0.69	NS
AF357355	317.33	388.00	0.82	0.99	0.87	NS
Snord110	297.33	158.00	1.88	1.00	0.62	NS
Snora24	271.51	742.24	0.37	1.00	0.07	NS
Z21	220.00	144.67	1.52	0.99	0.93	NS
Gm24148	198.00	134.00	1.48	1.00	0.78	NS
Snord22	189.33	340.00	0.56	1.00	0.24	NS
Snora52	180.00	212.67	0.85	1.00	0.42	NS
Snora16a	163.33	144.00	1.13	1.00	0.75	NS

with these snoRNAs, we transfected NIH3T3 fibroblasts with NXF3-GFP, NXF1-GFP, or GFP as control, immunoprecipitated with antibody to GFP, and we performed RT-qPCR on recovered RNA for abundant snoRNAs for which stem-loop primers were successfully designed. Each of the snoRNAs tested showed enrichment in NXF3-GFP pulldown over GFP pulldown (Fig. 3*B*). Most of these snoRNAs also associated with NXF1-GFP. Together, our data indicate that both NXF3 and NXF1 are capable of associating with a broad range of snoRNAs.

Knockdown and overexpression of NXF3 alters cytosolic Rpl13a snoRNAs in cardiomyoblasts

Although both NXF3 and NXF1 can associate with snoRNAs, only NXF3 conferred enhanced viability in our lipotoxicity screen in HUVECs. To compare the effects of NXF3 and NXF1 on snoRNA localization, we transfected H9c2 rat cardiomyoblasts with siRNAs to knock down either NXF3 or NXF1. Compared with control non-targeting siRNA, two independent siRNAs directed against NXF3 led to a 93 and 84% decrease in NXF3 mRNA levels, respectively, in cardiomyoblasts. NXF3 siRNAs were specific and did not significantly change levels of family member NXF1 (Fig. 4*A*, *left graph*). We found that commercially available antibodies directed against rodent NXF3 are not specific for this family member (data not shown), and our attempts to generate a specific antibody that recognizes the rat or murine protein were unsuccessful, thus precluding confirmation of the extent of knockdown of the endogenous NXF3 protein. Nonetheless, knockdown of NXF3 mRNA led to a 50–100% increase in cytosolic levels of the *Rpl13a* snoRNAs (Fig. 4*A*, *right graph*) without perturbing efficiency of fractionation (Fig. 4*B*). In contrast, siRNA knockdown of NXF1 had no effect on cytosolic levels of *Rpl13a* snoRNAs (Fig. 4, *C* and *D*). Thus, accumulation of *Rpl13a* snoRNAs in the cytosol can result from either acute or chronic knockdown of NXF3. This effect is consistent across different cell types (endothelial cells and cardiomyoblasts) and is not observed with knockdown of NXF1.

Our data are consistent with a model in which NXF3 function is required to maintain low cytoplasmic levels of the

Downloaded from http://www.jbc.org/ at Washington University on January 5, 2018

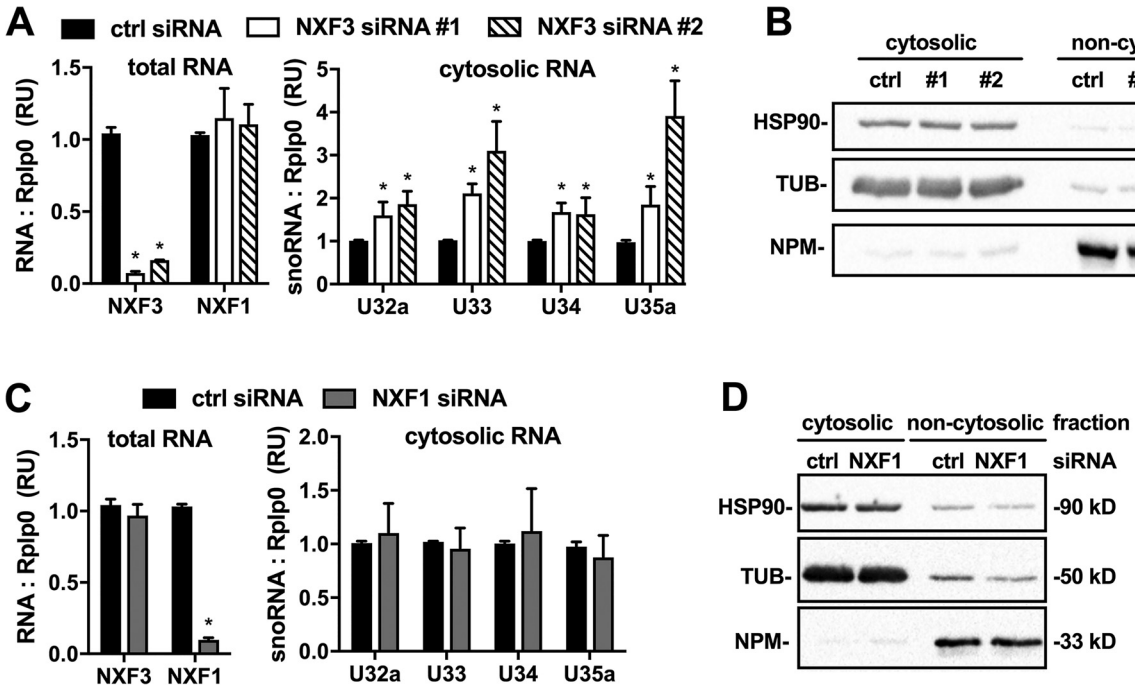

Figure 4. Knockdown of NXF3, but not NXF1, alters *Rpl13a* snoRNA localization. H9c2 cardiomyoblasts were transfected with scrambled siRNA (*ctrl*) or two independent siRNAs targeting NXF3 (*A* and *B*) or siRNAs targeting NXF1 (*C* and *D*). RT-qPCR quantification of NXF3 and NXF1 in total RNA (*A* and *C, left graphs*) and *Rpl13a* snoRNAs in cytosolic RNA (*A* and *C, right graphs*) for $n = 3$. Representative Western blot analysis (*B* and *D*) of cytosolic and non-cytosolic fractions for cytosolic (*HSP90* and *TUB*) and nuclear (*NPM*) markers as controls for *A* and *C*, respectively. Means ± S.D. *, $p < 0.05$ for NXF3 or NXF1 knockdown *versus* control.

Rpl13a snoRNAs. To test whether NXF3 promotes movement of snoRNAs between the cytosol and nucleus, we overexpressed murine NXF3 by transiently transfecting NIH3T3 murine fibroblasts with a GFP-tagged NXF3 construct (NXF3-GFP), a GFP-tagged NXF1 construct (NXF1-GFP), or a plasmid expressing GFP alone as control. We consistently observed more efficient transfection with GFP (76%) compared with NXF3-GFP (46%) or NXF1-GFP (40%), suggesting that endogenous mechanisms serve to restrict the overall expression of NXF3 and NXF1 (Fig. 5*A*). Nonetheless, compared with expression of GFP alone, expression of NXF3-GFP decreased cytosolic levels of the *Rpl13a* snoRNAs by 16–34%, whereas NXF1-GFP did not significantly change cytosolic levels (Fig. 5, *B* and *C*). Together with findings from knockdown of NXF3, our data suggest a model in which NXF3 specifically promotes movement of snoRNAs from the cytoplasm to the nucleus and determines the distribution of the snoRNAs between these cellular compartments.

Regulation of snoRNA trafficking and association with NXF3

Nucleocytoplasmic transport can serve as a point of regulation of subcellular localization for proteins as well as RNAs (24). Cyclic AMP is a potent regulator of protein trafficking, but it is not known whether this second messenger impacts NXF3 or snoRNA localization. We found that treatment of fibroblasts for 1 h with forskolin (FSK), an adenylyl cyclase activator, which increases cyclic AMP levels, significantly decreased cytosolic *Rpl13a* snoRNA levels compared with DMSO-treated controls (Fig. 6, *A* and *B*). To test whether FSK affects NXF3 localization or its association with snoRNAs, we transfected fibroblasts with a plasmid for expression of NXF3-GFP or NXF1-GFP. Similar to our findings with untransfected cells, cells overexpressing NXF3-GFP or NXF1-GFP had decreased cytosolic snoRNA abundance following 1 h of treatment with FSK (Fig. 6, *C–F*). Moreover, FSK increased association of NXF3-GFP with the *Rpl13a* snoRNAs (Fig. 7*A*). Concomitantly, immunofluorescence microscopy revealed increased nuclear localization of NXF3-GFP (Fig. 7*B*). By contrast FSK did not affect snoRNA association with NXF1-GFP or the cellular distribution of NXF1-GFP, which is predominantly nuclear (Fig. 7, *C* and *D*). Together, these observations are consistent with a model of NXF3-mediated trafficking of snoRNAs from the nucleus to the cytoplasm that is regulated by FSK. Moreover, these findings lend further specificity to the function of NXF3 in snoRNA trafficking.

To establish whether the FSK-induced changes in localization of *Rpl13a* snoRNAs are dependent on NXF3, cardiomyoblasts were transiently transfected with siRNA to knock down NXF3 (Fig. 8*A*) and then treated with FSK. Although FSK decreased cytosolic *Rpl13a* snoRNAs as expected in control siRNA-transfected cells, this effect was abrogated when NXF3 was knocked down with either of two independent siRNAs (Fig. 8*B*). In contrast, NXF1 siRNA knockdown had no effect on the FSK-snoRNA phenotype (Fig. 8*B*). Taken together, our data are most consistent with a model in which NXF3 plays a critical role in return of snoRNAs from the cytoplasm to the nucleus, a pathway that can be activated by FSK.

Discussion

The endogenous substrates for NXF3, a member of a family of RNA transport proteins, are not well-characterized. Additionally, relatively little is known regarding the regulation of distribution of snoRNAs between the nucleus and cytoplasm. Herein, we demonstrate that gain- and loss-of-function of

Downloaded from http://www.jbc.org/ at Washington University on January 5, 2018

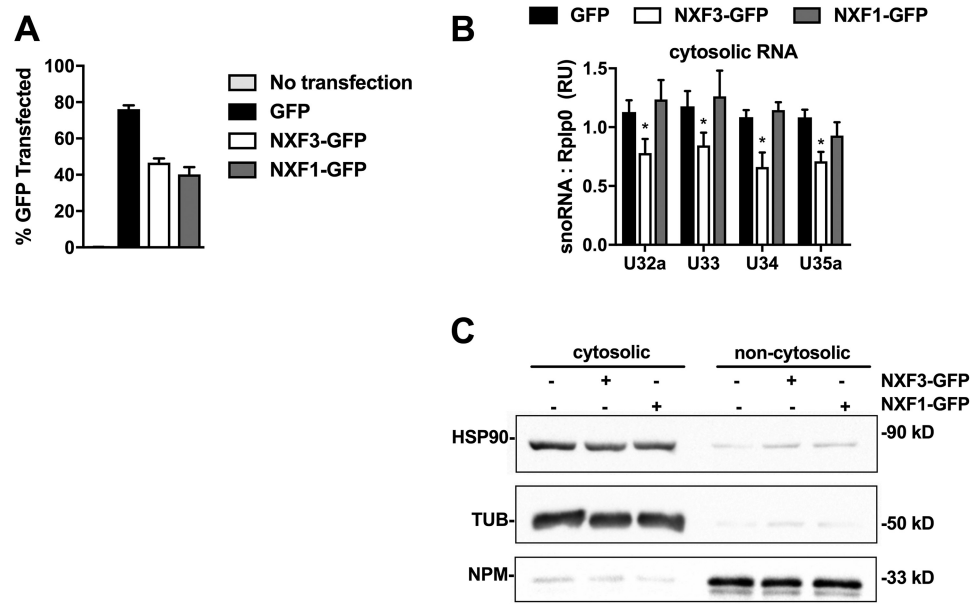

Figure 5. Overexpression of NXF3, but not NXF1, alters *Rpl13a* snoRNA localization in fibroblasts. NIH3T3 fibroblasts were transfected with control plasmid (*GFP*) or plasmids encoding NXF3-GFP or NXF1-GFP. *A,* flow cytometric analysis of transfected cells. $n = 3$. *B,* RT-qPCR of cytosolic *Rpl13a* snoRNAs for $n = 3$. *C,* representative Western blot analysis of cytosolic and non-cytosolic fractions for cytosolic (*HSP90* and *TUB*) and nuclear (*NPM*) markers. Means ± S.D. *, $p < 0.05$ for NXF3 knockdown *versus* control.

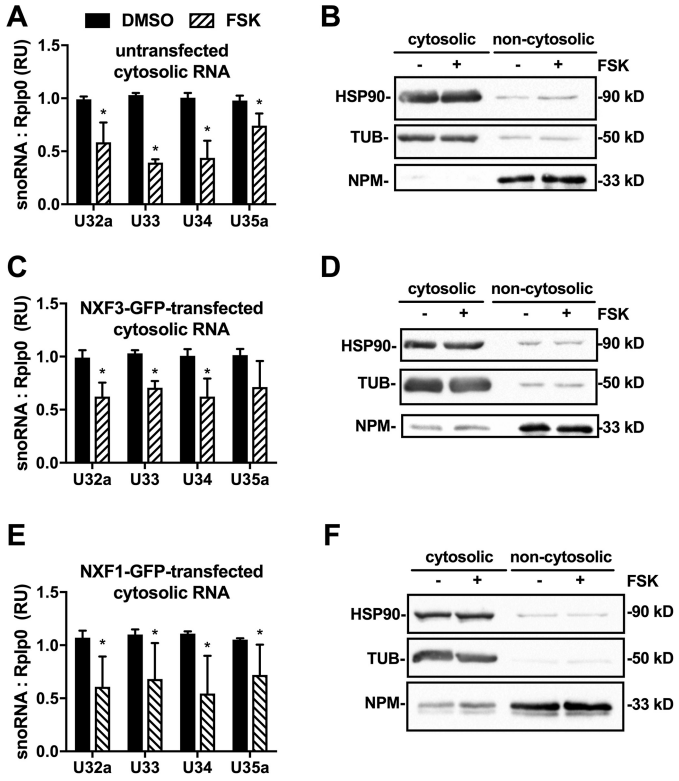

Figure 6. Forskolin decreases *Rpl13a* snoRNAs in cytoplasm. *A, C,* and *E,* untransfected NIH3T3 fibroblasts (*A*), cells transfected with NXF3-GFP (*C*), and cells transfected with NXF1-GFP (*E*) were treated with 10 μM FSK or vehicle (DMSO) for 1 h. Quantification of cytosolic snoRNAs relative to Rplp0. Means ± S.D. for $n = 3$. *, $p < 0.05$ for FSK *versus* DMSO. *B, D,* and *F,* representative Western blot analysis of cytosolic and non-cytosolic fractions for cytosolic (*HSP90* and *TUB*) and nuclear (*NPM*) markers for experiments in untransfected (*B*), NXF3-GFP-transfected (*D*), and NXF1-GFP-transfected (*F*) cells.

NXF3 alters subcellular distribution of snoRNAs encoded within the *Rpl13a* locus. Furthermore, we show that NXF3 associates with many box C/D and box H/ACA snoRNAs and regulates distribution of these small non-coding RNAs as a class. Our data are most consistent with a model in which snoRNAs cycle between the nucleus and cytoplasm and NXF3 efficiently imports snoRNAs from the cytoplasm to the nucleus, a function that helps to maintain low levels of snoRNAs in the cytoplasm under basal conditions (Fig. 9). Furthermore, we show that regulation of snoRNA distribution by FSK requires NXF3.

NXF family members have been identified based on sequence similarity and domain architecture that for most includes an amino-terminal containing RNA-binding protein interaction domain, a p15/NXT-heterodimerization domain, and a carboxyl-terminal domain involved in nuclear pore binding (25, 26). NXF1, NXF2, NXF3, and NXF5 have been shown to function in nuclear export of mRNAs, whereas NXF7 has been proposed to function in the cytoplasmic trafficking of mRNAs (15, 27–31). NXF3, which lacks carboxyl-terminal domains that function in nuclear export and nucleoporin binding, has a CRM1-dependent nuclear export sequence that allows it to partner with this transport receptor for its mRNA export function (15). Our study provides evidence that NXF3, but not NXF1, is also involved in transporting snoRNA cargos, expanding the functional repertoire of NXF proteins. Moreover, our data support a model in which NXF3 has a role in returning snoRNAs to the nucleus. Functional domains of NXF3 required for nuclear export of mRNA have been characterized (15, 26). However, nuclear localization sequences can be highly variable, and examination of the NXF3 sequence did not reveal motifs predicted with high likelihood to function in nuclear import, raising the possibility that NXF3 could function in a complex with other proteins. Our data provide evidence of a role for NXF3 in snoRNA transport. However, interaction of NXF3 with snoRNAs could be direct or indirect. In contrast to other NXF family members, RNA-binding domains of NXF3 are pre-

Downloaded from http://www.jbc.org/ at Washington University on January 5, 2018

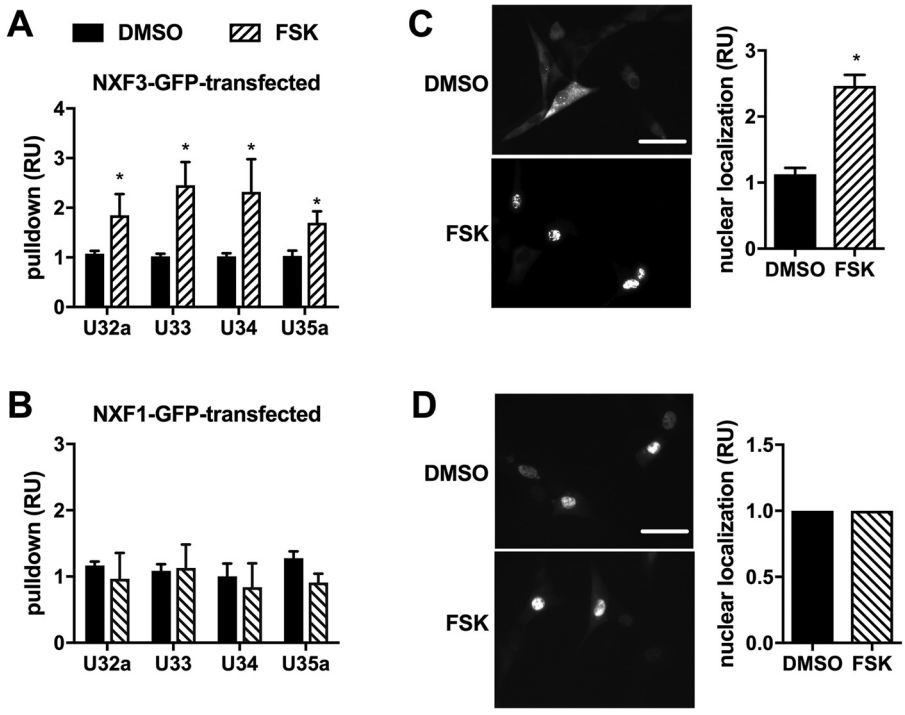

Figure 7. Forskolin increases NXF3-GFP-snoRNA association. *A* and *B*, NIH3T3 fibroblasts were transfected with plasmid encoding NXF3-GFP (*A*) or NXF1-GFP (*B*). Following treatment with FSK or vehicle (DMSO) for 1 h, *Rpl13a* snoRNAs immunoprecipitated with α-GFP were quantified by qPCR. *C* and *D*, representative immunofluorescence micrographs of NXF3-GFP-transfected (*C*) or NXF1-GFP-transfected (*D*) cells following 1 h of treatment with FSK or vehicle (DMSO). *Graphs* report the relative nuclear localization quantified from $n = 3$ independent experiments. *Scale bar*, 50 μM. Means ± S.D. for $n = 3$. *, $p < 0.05$ for FSK *versus* DMSO.

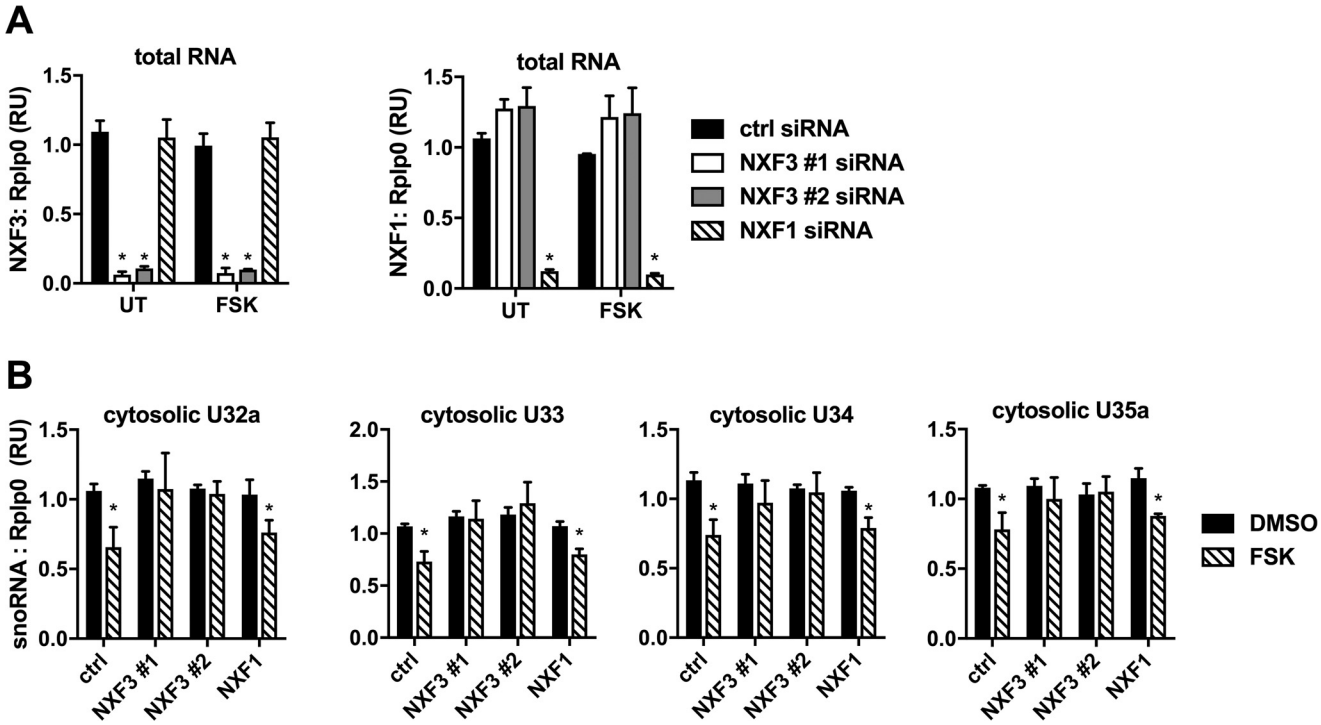

Figure 8. Forskolin effect on snoRNA localization is dependent on NXF3. H9c2 cardiomyoblasts were transfected with scrambled siRNA (*ctrl*) or two independent siRNAs targeting NXF3 or siRNA targeting NXF1 and subsequently treated for 1 h with 10 μM FSK or vehicle (DMSO). *A*, RT-qPCR quantification of total NXF3 and NXF1 relative to Rplp0. *B*, RT-qPCR quantification of cytosolic *Rpl13a* snoRNAs relative to Rplp0. Means ± S.D. for $n = 3$. *, $p < 0.05$ for FSK *versus* DMSO.

dicted but have not been functionally confirmed (32). In future studies, experimental delineation of RNA-binding residues in NXF3 will facilitate structure–function studies to determine whether this protein interacts directly with snoRNAs. In addition, future development of an *in vitro* nuclear transport assay for snoRNAs will help to test our model.

Downloaded from http://www.jbc.org/ at Washington University on January 5, 2018

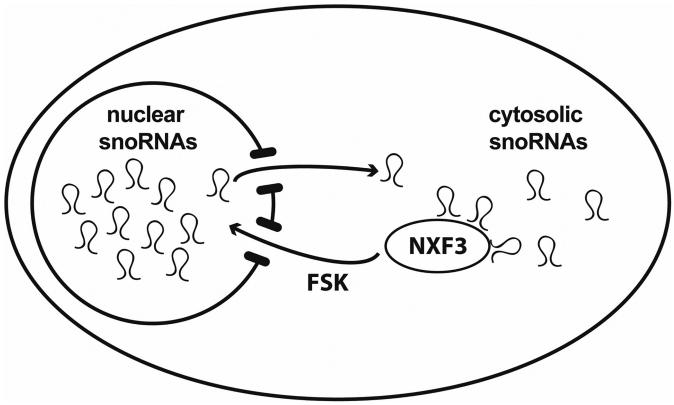

Figure 9. Model for NXF3 function in snoRNA localization. snoRNAs cycle between the nucleus and cytoplasm under homeostatic conditions. NXF3 functions as an importer, efficiently returning snoRNAs to the nucleus to maintain low snoRNA abundance in the cytoplasm relative to the nucleus. FSK treatment enhances return of NXF3–snoRNA complexes to the nucleus, further depleting cytosolic levels of snoRNAs.

Following transcription, snoRNAs that are processed from the introns of pre-mRNA or that are generated from independently transcribed units first move to Cajal bodies, where they assemble in to mature snoRNPs, and subsequently to the nucleolus, where they encounter nascent rRNA substrates. PHAX, a known adaptor for RNA export, is required for movement to the Cajal body, and CRM1, a nuclear export receptor, is required for movement to the nucleolus (33). A growing body of evidence indicates that snoRNAs traffic to the cytoplasm and extracellular space (8, 10–13, 34). Whether snoRNAs undergo processing in the cytoplasm analogous to snRNAs, function outside the nucleus, or are secreted in a regulated fashion remains to be determined. Nonetheless, cells maintain a gradient of snoRNAs such that the vast majority of endogenously expressed snoRNAs remain localized within the nucleus, and when exogenous snoRNAs are introduced into the cytoplasm, they are trafficked into the nucleus through the nuclear pore complex (14, 35). To date, PHAX and Snurportin 1 have been shown to function in nucleocytoplasmic trafficking of U8, an independently transcribed, capped box C/D snoRNA (11), but it is not known whether these proteins regulate the cytosolic trafficking of other snoRNAs. Our study provides the first demonstration of a transport protein that regulates cytoplasmic localization of snoRNAs as a class, including both box C/D and box H/ACA species, and it is likely functioning to return cytoplasmic snoRNAs to the nucleus. Inhibition of CRM1 function with leptomycin B decreased, rather than increased, cytosolic snoRNA abundance,[3] suggesting that in contrast to the mRNA export function of NXF3, NXF3-mediated return of snoRNAs to the nucleus may be independent of this transport co-receptor.

Transport of RNAs between the nucleus and cytoplasm is a highly regulated process, and our studies provide new evidence that FSK regulates the association of snoRNAs and the transport protein, NXF3, as well as the trafficking of both snoRNAs and NXF3. Although it is possible that FSK-induced translocation of NXF3 leads to increased association with snoRNAs that are concentrated in the nucleus, our data establish that NXF3 is required for acute regulation of nuclear snoRNA import by FSK. FSK is a natural compound that activates cyclic AMP signaling through both PKA-dependent and PKA-independent mechanisms (36–39). This could lead to altered post-translational modifications, such as phosphorylation of NXF3 or other proteins that function in snoRNA transport. Although examination of the NXF3 primary sequence suggests a number of potential phosphorylation sites, FSK did not change NXF3 phosphorylation, as determined using a panel of α-phosphotyrosine, α-phosphoserine, and α-phosphothreonine antibodies.[3] It is possible that the available antibodies lack the appropriate specificity or that NXF3 is not a direct target of FSK. Future structure–function and mass spectrometry studies will be necessary to address these possibilities.

Knockdown of NXF3 confers resistance to lipotoxicity, a process dependent on snoRNAs from the *Rpl13a* locus. These non-coding RNAs accumulate in the cytoplasm early during lipotoxicity (10, 17, 19). Loss of NXF3 also alters distribution of these snoRNAs at baseline and prevents the acute increase in cytosolic levels with lipotoxicity. The abundance of cytoplasmic *Rpl13a* snoRNAs in NXF3-knockdown cells is comparable with the levels achieved in control cells following acute lipotoxic exposure. This suggests that the dynamic change in cytosolic snoRNAs, rather than the absolute cytoplasmic levels of these non-coding RNAs, is a key contributor to lipotoxic injury.

Recent genetic studies and identification of diseases associated with dysregulation of snoRNAs have expanded the biological repertoire for snoRNAs beyond their well-appreciated canonical role in modification of nascent rRNAs (9, 40, 41). Although it is certainly possible that dynamic changes in snoRNA-directed rRNA modifications contribute to these intriguing phenotypes, localization of snoRNAs in the cytoplasm also raises the possibility that non-canonical snoRNA functions are mediated through effects on novel targets outside the nucleolus. A complete understanding of this new snoRNA biology requires further dissection of snoRNA trafficking and its regulation. Our identification of a role for NXF3 in regulated snoRNA trafficking represents a first step in this important direction.

Experimental procedures

Materials

Digitonin, FSK, phenylmethanesulfonyl fluoride (PMSF), and dimethyl sulfoxide (DMSO) were from Sigma. Protein A Dynabeads and TURBO DNase were from Thermo Fisher Scientific. Doxorubicin (DOX) was from Cayman Chemical. TRIzol LS and SUPERase-IN RNase inhibitor was from Life Technologies, Inc. DTT was from Calbiochem, and β-mercaptoethanol was from Sigma. Laemmli Sample Buffer was from Bio-Rad.

Plasmids

The NXF3 cDNA was obtained from the Sun lab (42) and cloned into pEGFP-C1 (Clontech) at BamHI and SalI sites. The full-length cDNA for mouse NXF1 was obtained by PCR from the total RNA of NIH3T3 mouse fibroblasts using primers containing BamHI and SalI restrictions sites. NXF1 cDNA was

[3] M. W. Li, and J. E. Schaffer, unpublished data.

Downloaded from http://www.jbc.org/ at Washington University on January 5, 2018

cloned into pEGFP-C1 (Clontech) at BamHI and SalI sites. PCR-derived sequences were confirmed by DNA sequencing.

Cells

H9c2 cardiomyoblasts and NIH3T3 fibroblasts were from American Type Culture Collection. Telomerase-immortalized HUVECs were a gift from Judah Folkman's laboratory (Harvard Medical School) (43), and H9c2 and 3T3 cells were maintained in Dulbecco's modified Eagle's medium (DMEM) with 10% heat-inactivated fetal bovine serum (H9c2) or 10% calf serum (NIH3T3). HUVECs were maintained in endothelial cell growth medium (Lonza). DOX (20 μM for 1 h), FSK (10 μM for 1 h), H_2O_2 (1 mM, 4 h), or palmitate (500 μM) was added to media as indicated. Cell viability was determined using CellTiter-Glo Luminescent Cell Viability Assay (Promega). Basal cellular ROS was detected by staining cells (100,000 cells per well of 12-well dishes) with 10 μM dihydroethidium (DHE) (Thermo Fisher Scientific) and detection using a microplate fluorescence reader (Tecan). ROS after palmitate treatment was detected by staining cells (200,000 cells per well of 6-cm dishes) with CellROX Deep Red Reagent (5 μM, 30 min) (Thermo Fisher Scientific) and detection using flow cytometric analysis on 10^4 cells/sample. Cells were transfected with plasmid DNA peGFP-1, NXF3-GFP, and NXF1-GFP using Lipofectamine 2000 (Life Technologies, Inc.) and with siRNAs (Life Technologies, Inc., Silencer Select) using RNAiMax (Life Technologies, Inc.), according to the manufacturers' protocols. Flow cytometric analysis of transfected cells assessed fluorescence on 10^4 cells/sample.

shRNA screen

The shRNA screen was performed using Decode Pooled Lentiviral shRNA Libraries by Thermo Fisher Scientific. Immortalized HUVECs were transduced with lentiviral shRNA pools at a multiplicity of infection of 0.1 and then selected using puromycin. Puromycin-resistant cells were then treated with 500 μM palmitate for 48 h. After removing palmitate, cells were grown to form colonies in normal media. Colonies were hand-picked and re-tested for viability following lipotoxic exposure. For this, cells were plated in a 96-well plate in triplicate (1000 cells per well) and treated with 500 μM palmitate for 24 h. Cells transduced with non-targeting shRNA viral particles (designed to not target mRNAs in the mammalian genome) were used as negative control. Colonies with significantly greater viability than control cells were selected for further analysis. Genomic DNA was isolated from palmitate-resistant cells, and PCR was used to amplify barcodes corresponding to specific shRNAs for sequencing. Sequences were compared with the Decode shRNA libraries or analyzed using BLAST to identify the knocked down genes.

Subcellular fractionation

For fractionation by detergent extraction, cell pellets were incubated in digitonin buffer (150 mM NaCl, 50 mM HEPES, pH 7.4, 100 μg/ml digitonin, 5 mM EDTA, and 0.1 unit/μl SUPERase-In RNase inhibitor) for 10 min and centrifuged for 10 min at 2000 $\times$ *g* to yield a cytoplasmic supernatant and non-cytoplasmic pellet containing membranes and nuclei (44).

RNA isolation and quantitative real-time PCR

Total RNA was isolated from cytoplasmic or non-cytoplasmic fractions and from immunoprecipitates using TRIzol LS according to manufacturer's protocol (Life Technologies, Inc.). cDNA was synthesized with SuperScript III first-strand synthesis system (Invitrogen) using oligo(dT) priming for mRNAs and target-specific stem-loop priming snoRNAs (10). qPCR was performed using PerfeCTa SYBR Green SuperMix (Quantabio). Relative quantitation of target transcript expression was calculated using the dd*CT* method using Rplp0 as an endogenous control on an ABI 7500 fast real-time PCR system.

Immunoprecipitation

Cells were sonicated in 50 mM Tris, pH 8.0, 150 mM NaCl, 2 mM EDTA, 0.5% Nonidet P-40 containing 1$\times$ cOmplete protease inhibitor mixture (Sigma), 1 mM PMSF, and 0.1 unit/μl RNase inhibitor SUPERase-In. After treatment with 0.3 units/μl TURBO DNase, insoluble material was removed by centrifugation at 20,000 $\times$ *g* for 10 min at 4 °C. Lysate was incubated with α-GFP (2.5 mg/ml) and protein A Dynabeads for 4 h at 4 °C. Complexes were washed four times with lysis buffer. For Western blot analysis, protein was eluted by incubation in Laemmli Sample Buffer, and RNA was eluted by incubation in TRIzol LS.

RNA sequencing

Input and immunoprecipitated RNA from three independent experiments was isolated and concentrated using RNA Clean and Concentrator-5 (Zymo Research). Indexed RNA-sequencing libraries were made using the Illumina TruSeq small RNA kit. Libraries were amplified with 14 cycles of PCR, pooled, and separated by PAGE. Products with sizes 30–375 nucleotides were excised and collected from the gel. Sequencing was performed using an Illumina HiSeq 2500. Demultiplexed data were analyzed using Partek Flow (build version 6.0.17.0305 Copyright ©; 2017 Partek Inc., St. Louis, MO). Sequences were evaluated for quality and trimmed to remove adaptor sequence. A custom Linux script was used to remove murine ribosomal sequences according to the Illumina iGenome murine genome annotation. Remaining sequences were aligned to the murine genome (mm9 Refseq Transcript August 1, 2016, Bowtie for Illumina, default settings), and aligned reads were quantified, normalized, and annotated. Analysis was limited to genes with >100 aligned reads. A step-up false discovery rate of 0.05 was considered significant. Sequence data have been deposited in NCBI's Gene Expression Omnibus (accession number GSE106301).

Immunoblots

Protein in total, cytoplasmic, and non-cytoplasmic fractions was quantified by bicinchoninic assay (Thermo Fisher Scientific), separated by SDS-PAGE, and immunoblotted. Detection for human nuclear export factor 3 (NXF3; Abcam ab76430, 1:500), GFP (Abcam ab290, 1:5000), heat-shock protein 90 (HSP90; Enzo SPA-846, 1:1000), α-tubulin (Sigma T6199, 1:2000), and nucleophosmin (NPM; Abcam ab37659, 1:1500) used horseradish peroxidase-conjugated secondary antibodies (Jackson ImmunoResearch) and Western Lightning Plus-ECL (PerkinElmer Life Sciences) using a ChemiDoc Imaging System.

Downloaded from http://www.jbc.org/ at Washington University on January 5, 2018

Immunofluorescence

Cells were grown on glass coverslips coated with 0.8% gelatin, fixed with 4% paraformaldehyde, permeabilized with Nonidet P-40, and blocked with 200 μg/ml ChromPure IgG (Jackson ImmunoResearch) corresponding to secondary antibody species. Detection for NPM used α-NPM (Life Technologies, Inc., 325200; 1:1000) with secondary Alexa Fluor 350 donkey anti-mouse IgG (Life Technologies, Inc., A10035; 40 μg/ml). GFP transfected cells were grown on glass coverslips and fixed with 4% paraformaldehyde. Coverslips were mounted on microscope slides using SlowFade Antifade reagent (Life Technologies, Inc., S2828). Slides were imaged on a Zeiss Axioskop 2 mot plus microscope with a Zeiss AxioCam MRm camera with a ×40 oil immersion objective at room temperature. Images were acquired using AxioVision Rel. 4.8 software. Images were processed identically using the ImageJ software package.

Statistics

Biochemical results are presented as mean ± S.D. for a minimum of three independent experiments. Statistical significance was assessed by two-tailed unpaired *t* test. p value < 0.05 was considered significant.

Author contributions—M. W. L., A. C. S., and K. D. P. performed cell culture and RNA-sequencing experiments. J. L. performed genetic screening. M. W. L. and S. J. M. analyzed RNA-sequencing results. D. S. O. and J. E. S. conceived and coordinated the studies and supervised the experiments. All authors reviewed the results, and M. W. L. wrote the paper. All authors approved the final version of the manuscript.

Acknowledgments—We thank the Genome Technology Access Center at the Department of Genetics, Washington University School of Medicine, for help with RNA-sequencing. The Center is partially supported by NCI Cancer Center Support Grant P30 CA91842 to the Siteman Cancer Center and by ICTS/CTSA Grant UL1 TR000448 from the NCRR, National Institutes of Health, and National Institutes of Health Roadmap for Medical Research.

References

1. Filipowicz, W., and Pogacić, V. (2002) Biogenesis of small nucleolar ribonucleoproteins. *Curr. Opin. Cell Biol.* **14,** 319–327
2. Kiss, T. (2004) Biogenesis of small nuclear RNPs. *J. Cell Sci.* **117,** 5949–5951
3. Matera, A. G., Terns, R. M., and Terns, M. P. (2007) Non-coding RNAs: lessons from the small nuclear and small nucleolar RNAs. *Nat. Rev. Mol. Cell Biol.* **8,** 209–220
4. Ender, C., Krek, A., Friedländer, M. R., Beitzinger, M., Weinmann, L., Chen, W., Pfeffer, S., Rajewsky, N., and Meister, G. (2008) A human snoRNA with microRNA-like functions. *Mol. Cell* **32,** 519–528
5. Kishore, S., Khanna, A., Zhang, Z., Hui, J., Balwierz, P. J., Stefan, M., Beach, C., Nicholls, R. D., Zavolan, M., and Stamm, S. (2010) The snoRNA MBII-52 (SNORD 115) is processed into smaller RNAs and regulates alternative splicing. *Hum. Mol. Genet.* **19,** 1153–1164
6. Schwartz, S., Bernstein, D. A., Mumbach, M. R., Jovanovic, M., Herbst, R. H., León-Ricardo, B. X., Engreitz, J. M., Guttman, M., Satija, R., Lander, E. S., Fink, G., and Regev, A. (2014) Transcriptome-wide mapping reveals widespread dynamic-regulated pseudouridylation of ncRNA and mRNA. *Cell* **159,** 148–162
7. Vitali, P., Basyuk, E., Le Meur, E., Bertrand, E., Muscatelli, F., Cavaillé, J., and Huttenhofer, A. (2005) ADAR2-mediated editing of RNA substrates in the nucleolus is inhibited by C/D small nucleolar RNAs. *J. Cell Biol.* **169,** 745–753
8. Holley, C. L., Li, M. W., Scruggs, B. S., Matkovich, S. J., Ory, D. S., and Schaffer, J. E. (2015) Cytosolic accumulation of small nucleolar RNAs (snoRNAs) is dynamically regulated by NADPH oxidase. *J. Biol. Chem.* **290,** 11741–11748
9. Lee, J., Harris, A. N., Holley, C. L., Mahadevan, J., Pyles, K. D., Lavagnino, Z., Scherrer, D. E., Fujiwara, H., Sidhu, R., Zhang, J., Huang, S. C., Piston, D. W., Remedi, M. S., Urano, F., Ory, D. S., and Schaffer, J. E. (2016) Rpl13a small nucleolar RNAs regulate systemic glucose metabolism. *J. Clin. Invest.* **126,** 4616–4625
10. Michel, C. I., Holley, C. L., Scruggs, B. S., Sidhu, R., Brookheart, R. T., Listenberger, L. L., Behlke, M. A., Ory, D. S., and Schaffer, J. E. (2011) Small nucleolar RNAs U32a, U33, and U35a are critical mediators of metabolic stress. *Cell Metab.* **14,** 33–44
11. Watkins, N. J., Lemm, I., and Lührmann, R. (2007) Involvement of nuclear import and export factors in U8 box C/D snoRNP biogenesis. *Mol. Cell Biol.* **27,** 7018–7027
12. Youssef, O. A., Safran, S. A., Nakamura, T., Nix, D. A., Hotamisligil, G. S., and Bass, B. L. (2015) Potential role for snoRNAs in PKR activation during metabolic stress. *Proc. Natl. Acad. Sci. U.S.A.* **112,** 5023–5028
13. Sienna, N., Larson, D. E., and Sells, B. H. (1996) Altered subcellular distribution of U3 snRNA in response to serum in mouse fibroblasts. *Exp. Cell Res.* **227,** 98–105
14. Baserga, S. J., Gilmore-Hebert, M., and Yang, X. W. (1992) Distinct molecular signals for nuclear import of the nucleolar snRNA, U3. *Genes Dev.* **6,** 1120–1130
15. Yang, J., Bogerd, H. P., Wang, P. J., Page, D. C., and Cullen, B. R. (2001) Two closely related human nuclear export factors utilize entirely distinct export pathways. *Mol. Cell* **8,** 397–406
16. Yang, J., Bardes, E. S., Moore, J. D., Brennan, J., Powers, M. A., and Kornbluth, S. (1998) Control of cyclin B1 localization through regulated binding of the nuclear export factor CRM1. *Genes Dev.* **12,** 2131–2143
17. Caputa, G., Zhao, S., Criado, A. E., Ory, D. S., Duncan, J. G., and Schaffer, J. E. (2016) RNASET2 is required for ROS propagation during oxidative stress-mediated cell death. *Cell Death Differ.* **23,** 347–357
18. Yang, K., Wang, M., Zhao, Y., Sun, X., Yang, Y., Li, X., Zhou, A., Chu, H., Zhou, H., Xu, J., Wu, M., Yang, J., and Yi, J. (2016) A redox mechanism underlying nucleolar stress sensing by nucleophosmin. *Nat. Commun.* **7,** 13599
19. Scruggs, B. S., Michel, C. I., Ory, D. S., and Schaffer, J. E. (2012) SmD3 regulates intronic non-coding RNA biogenesis. *Mol. Cell Biol.* **32,** 4092–4103
20. Shanker, S., Paulson, A., Edenberg, H. J., Peak, A., Perera, A., Alekseyev, Y. O., Beckloff, N., Bivens, N. J., Donnelly, R., Gillaspy, A. F., Grove, D., Gu, W., Jafari, N., Kerley-Hamilton, J. S., Lyons, R. H., Tepper, C., and Nicolet, C. M. (2015) Evaluation of commercially available RNA amplification kits for RNA sequencing using very low input amounts of total RNA. *J. Biomol. Tech.* **26,** 4–18
21. Dupuis-Sandoval, F., Poirier, M., and Scott, M. S. (2015) The emerging landscape of small nucleolar RNAs in cell biology. *Wiley Interdiscip. Rev. RNA* **6,** 381–397
22. Fasold, M., Langenberger, D., Binder, H., Stadler, P. F., and Hoffmann, S. (2011) DARIO: a ncRNA detection and analysis tool for next-generation sequencing experiments. *Nucleic Acids Res.* **39,** W112–W117
23. Lestrade, L., and Weber, M. J. (2006) snoRNA-LBME-db, a comprehensive database of human H/ACA and C/D box snoRNAs. *Nucleic Acids Res.* **34,** D158–D162
24. Nigg, E. A. (1997) Nucleocytoplasmic transport: signals, mechanisms and regulation. *Nature* **386,** 779–787
25. Izaurralde, E. (2001) Friedrich Mieschер Prize awardee lecture review. A conserved family of nuclear export receptors mediates the exit of messenger RNA to the cytoplasm. *Cell. Mol. Life Sci.* **58,** 1105–1112
26. Sasaki, M., Takeda, E., Takano, K., Yomogida, K., Katahira, J., and Yoneda, Y. (2005) Molecular cloning and functional characterization of mouse Nxf family gene products. *Genomics* **85,** 641–653

Downloaded from http://www.jbc.org/ at Washington University on January 5, 2018

27. Jun, L., Frints, S., Duhamel, H., Herold, A., Abad-Rodrigues, J., Dotti, C., Izaurralde, E., Marynen, P., and Froyen, G. (2001) NXF5, a novel member of the nuclear RNA export factor family, is lost in a male patient with a syndromic form of mental retardation. *Curr. Biol.* **11,** 1381–1391
28. Kang, Y., and Cullen, B. R. (1999) The human Tap protein is a nuclear mRNA export factor that contains novel RNA-binding and nucleocytoplasmic transport sequences. *Genes Dev.* **13,** 1126–1139
29. Katahira, J., Miki, T., Takano, K., Maruhashi, M., Uchikawa, M., Tachibana, T., and Yoneda, Y. (2008) Nuclear RNA export factor 7 is localized in processing bodies and neuronal RNA granules through interactions with shuttling hnRNPs. *Nucleic Acids Res.* **36,** 616–628
30. Kuersten, S., Segal, S. P., Verheyden, J., LaMartina, S. M., and Goodwin, E. B. (2004) NXF-2, REF-1, and REF-2 affect the choice of nuclear export pathway for tra-2 mRNA in *C. elegans*. *Mol. Cell* **14,** 599–610
31. Tretyakova, I., Zolotukhin, A. S., Tan, W., Bear, J., Propst, F., Ruthel, G., and Felber, B. K. (2005) Nuclear export factor family protein participates in cytoplasmic mRNA trafficking. *J. Biol. Chem.* **280,** 31981–31990
32. Herold, A., Suyama, M., Rodrigues, J. P., Braun, I. C., Kutay, U., Carmo-Fonseca, M., Bork, P., and Izaurralde, E. (2000) TAP (NXF1) belongs to a multigene family of putative RNA export factors with a conserved modular architecture. *Mol. Cell. Biol.* **20,** 8996–9008
33. Boulon, S., Verheggen, C., Jady, B. E., Girard, C., Pescia, C., Paul, C., Ospina, J. K., Kiss, T., Matera, A. G., Bordonné, R., and Bertrand, E. (2004) PHAX and CRM1 are required sequentially to transport U3 snoRNA to nucleoli. *Mol. Cell* **16,** 777–787
34. Lefebvre, F. A., Benoit Bouvrette, L. P., Perras, L., Blanchet-Cohen, A., Garnier, D., Rak, J., and Lécuyer, É. (2016) Comparative transcriptomic analysis of human and *Drosophila* extracellular vesicles. *Sci. Rep.* **6,** 27680
35. Michaud, N., and Goldfarb, D. (1992) Microinjected U snRNAs are imported to oocyte nuclei via the nuclear pore complex by three distinguishable targeting pathways. *J. Cell Biol.* **116,** 851–861
36. Namkoong, S., Kim, C. K., Cho, Y. L., Kim, J. H., Lee, H., Ha, K. S., Choe, J., Kim, P. H., Won, M. H., Kwon, Y. G., Shim, E. B., and Kim, Y. M. (2009) Forskolin increases angiogenesis through the coordinated cross-talk of PKA-dependent VEGF expression and Epac-mediated PI3K/Akt/eNOS signaling. *Cell. Signal.* **21,** 906–915
37. Galli, C., Meucci, O., Scorziello, A., Werge, T. M., Calissano, P., and Schettini, G. (1995) Apoptosis in cerebellar granule cells is blocked by high KCl, forskolin, and IGF-1 through distinct mechanisms of action: the involvement of intracellular calcium and RNA synthesis. *J. Neurosci.* **15,** 1172–1179
38. Hoque, K. M., Woodward, O. M., van Rossum, D. B., Zachos, N. C., Chen, L., Leung, G. P., Guggino, W. B., Guggino, S. E., and Tse, C. M. (2010) Epac1 mediates protein kinase A-independent mechanism of forskolin-activated intestinal chloride secretion. *J. Gen. Physiol.* **135,** 43–58
39. Delghandi, M. P., Johannessen, M., and Moens, U. (2005) The cAMP signalling pathway activates CREB through PKA, p38, and MSK1 in NIH3T3 cells. *Cell. Signal.* **17,** 1343–1351
40. Jenkinson, E. M., Rodero, M. P., Kasher, P. R., Uggenti, C., Oojageer, A., Goosey, L. C., Rose, Y., Kershaw, C. J., Urquhart, J. E., Williams, S. G., Bhaskar, S. S., O'Sullivan, J., Baerlocher, G. M., Haubitz, M., Aubert, G., *et al.* (2016) Mutations in SNORD118 cause the cerebral microangiopathy leukoencephalopathy with calcifications and cysts. *Nat. Genet.* **48,** 1185–1192
41. Siprashvili, Z., Webster, D. E., Johnston, D., Shenoy, R. M., Ungewickell, A. J., Bhaduri, A., Flockhart, R., Zarnegar, B. J., Che, Y., Meschi, F., Puglisi, J. D., and Khavari, P. A. (2016) The non-coding RNAs SNORD50A and SNORD50B bind K-Ras and are recurrently deleted in human cancer. *Nat. Genet.* **48,** 53–58
42. Yin, Y., Wang, G., Liang, N., Zhang, H., Liu, Z., Li, W., and Sun, F. (2013) Nuclear export factor 3 is involved in regulating the expression of TGF-β3 in an mRNA export activity-independent manner in mouse Sertoli cells. *Biochem. J.* **452,** 67–78
43. Freedman, D. A., and Folkman, J. (2004) Maintenance of G1 checkpoint controls in telomerase-immortalized endothelial cells. *Cell Cycle* **3,** 811–816
44. Holden, P., and Horton, W. A. (2009) Crude subcellular fractionation of cultured mammalian cell lines. *BMC Res. Notes* **2,** 243

Downloaded from http://www.jbc.org/ at Washington University on January 5, 2018

Nuclear export factor 3 regulates localization of small nucleolar RNAs

Melissa W. Li, Arthur C. Sletten, Jiyeon Lee, Kelly D. Pyles, Scot J. Matkovich, Daniel S. Ory and Jean E. Schaffer

J. Biol. Chem. 2017, 292:20228-20239.
doi: 10.1074/jbc.M117.818146 originally published online October 11, 2017

Access the most updated version of this article at doi: 10.1074/jbc.M117.818146

Alerts:
- When this article is cited
- When a correction for this article is posted

Click here to choose from all of JBC's e-mail alerts

This article cites 44 references, 15 of which can be accessed free at
http://www.jbc.org/content/292/49/20228.full.html#ref-list-1

Downloaded from http://www.jbc.org/ at Washington University on January 5, 2018